JOC The Journal of Organic Chemistry

pubs.acs.org/joc Article

Temporal Control of the Host–Guest Properties of a Calix[6]arene Receptor by the Use of a Chemical Fuel

Francesco Rispoli,[§] Emanuele Spatola,[§] Daniele Del Giudice,[§] Roberta Cacciapaglia, Alessandro Casnati, Laura Baldini,* and Stefano Di Stefano*

Cite This: J. Org. Chem. 2022, 87, 3623–3629 Read Online

ACCESS | Metrics & More | Article Recommendations | Supporting Information

ABSTRACT: The host–guest interaction of a 1,3,5-trisaminocalix[6]arene receptor with *N*-methylisoquinolinium trifluoromethanesulfonate (K_{ass} of 500 ± 30 M^{-1} in CD_2Cl_2) can be dissipatively driven by means of 2-cyano-2-(4′-chloro)-phenylpropanoic acid used as a convenient chemical fuel. When the fuel is added to a dichloromethane solution containing the above complex, the host is induced to immediately release the guest in the bulk solution. Consumption of the fuel allows the guest to be re-uptaken by the host. The operation can be satisfactorily reiterated with four subsequent additions of fuel, producing four successive release–reuptake cycles. The percentage of the guest temporarily released in the bulk solution by the host and the time required for the reuptake process can be finely regulated by varying the quantities of added fuel.

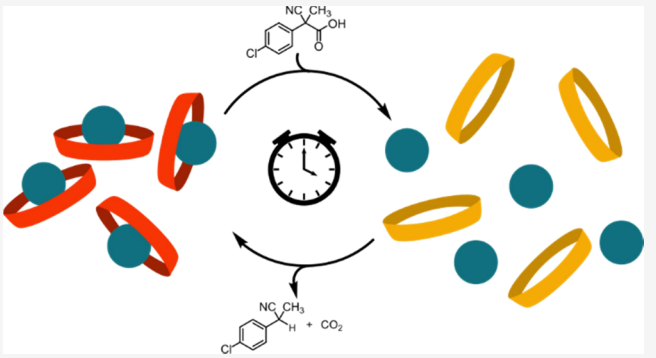

INTRODUCTION

The capability of maintaining a functional state under the action of a chemical or photochemical stimulus is probably the characterizing feature of any chemical system with life-like properties.[1] For this reason, a great effort is nowadays devoted to the design of artificial machineries that operate under dissipative conditions, that is until the stimulus (fuel) is present.[1a,2] A number of dissipative systems have been recently developed in the fields of self-assembly,[3] DNA-based systems,[4] molecular machines and pumps,[1a,2,5] and host–guest chemistry,[6] with a clear predominance of the first category. In the case of dissipative host–guest chemistry, in 2015, Nitschke et al.[6a] described the release–reuptake of a fullerene guest from and to a metal–organic architecture that disassembled and reassembled under the action of a chemical fuel (thus, in this case, the identity of the host is lost during the release phase); in 2021, we reported[6b] on the temporal control of alpha-cyclodextrin–*para*-aminobenzoic acid interactions driven by programmed pH variations enabled by the consumption of the nitroacetic acid fuel, and Schmittel et al. described a system in which a secondary ammonium/amino axis is dissipatively hosted inside the cavity of a crown-ether derivative.[7]

In the last years, activated carboxylic acids like 2-cyano-2-phenylpropanoic acid[8] (**1a**) and its derivatives (**1b–d**),[9] trichloroacetic acid,[10] and nitroacetic acid[4i] (Chart 1) have been conveniently used as chemical fuels to drive whole cycles of motion of molecular machines, both switches and motors. Very recently, we reported that the calix[4]arene scaffold of **2** (Figure 1) can be reversibly locked and unlocked in a time-controlled fashion by means of acids **1a–d** used as chemical fuels.[9c]

Chart 1. Activated carboxylic acids employed for the operation of molecular machines.

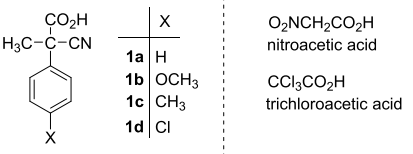

The two amino groups implanted on the opposite positions of the upper rim of calix[4]arene **2** allow the locking/unlocking motion. It was demonstrated that such $-NH_2$ groups share the proton received by the fuel acid, with a consequent locking of the structure (locked states **B′** and **B″**, see Figure 1). The locked shape is maintained until the decarboxylation of the fuel acid is complete (fuel exhaustion). At this point, the calix[4]arene is found again in its unlocked form **A** (Figure 1).

Received: January 10, 2022
Published: February 23, 2022

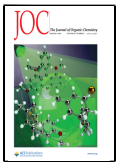

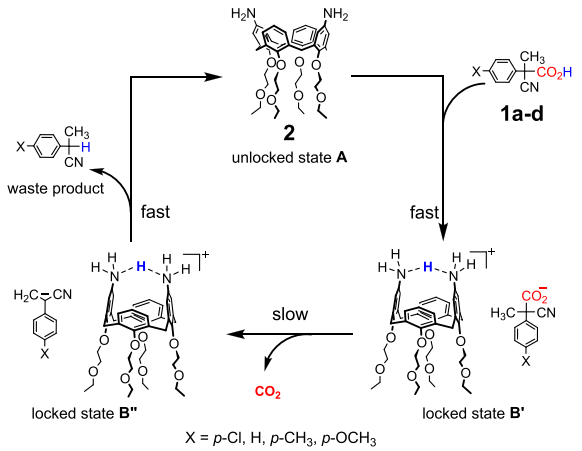

Figure 1. Locking−unlocking of the calix[4]arene scaffold of compound **2**, due to the action of the fuel acid, which loses CO_2 during the operation. The system operates in dichloromethane.

Most importantly, it was demonstrated that the duration of the locking/unlocking conformational cycle can be controlled by varying the nature of the fuel acid (increasing times in the series X = Cl, H, CH_3, and OCH_3) or the amount of added fuel (the greater the excess of added fuel with respect to the calix[4]arene, the longer the duration of the conformational cycle).[9c] Subsequently, such study has found application in the temporal control of the fluorescence properties of a similar diaminocalix[4]arene further endowed with two pyrenyl moieties on the remaining opposite positions of the upper rim.[10b]

We now resort to the calix[6]arene **3** (see Figure 2) where three alternate aromatic moieties are functionalized with three

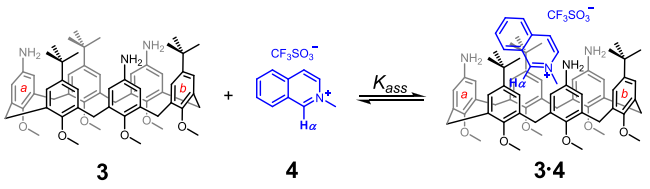

Figure 2. Host−guest interaction between calix[6]arene **3** and *N*-methylisoquinolinium trifluoromethanesulfonate (**4**).

amine groups. Although floppier and less organized than the calix[4]arene scaffold, the calix[6]arene cavity is larger and potentially capable of hosting guest molecules.[11] Our purpose is to drive in a temporally controlled fashion the host−guest interactions between host **3** and a suitable guest molecule by means of carboxylic acid fuels under dissipative conditions. Time control of the protonation state of the amino groups of **3** should allow the dissipative release−reuptake of the guest.

RESULTS AND DISCUSSION

Synthesis. Synthesis of compound **3**[12] was attained in four steps from 1,3,5-trimethoxycalix[6]arene[13] following a literature procedure.[12] Compound **4**[14] was prepared as previously described.

Binding and Base Properties of 3. A significant portion of the ^{1}H-NMR (300 MHz) spectrum in CD_2Cl_2 at 25 °C of **3** is reported as the trace *a* of Figure 3 (see bottom trace in Figure S2, in the Supporting Information for the entire spectrum). The two singlets at 3.0 and 3.6 ppm correspond to the methoxy groups, while the singlet at 3.8 ppm is due to the 12 protons of the methylene bridges. Singlets at 6.0 ppm and 7.2 ppm are due to the aromatic protons of rings *a* and *b*, respectively.

The presence of a single singlet for the protons of the methylenic bridges indicates that calix[6]arene **3** is conformationally flexible,[15] due to a fast rotation of the aromatic rings around the methylene hinges on the NMR time-scale. With the aim at testing *N*-methylisoquinolinium trifluoromethanesulfonate **4** as a suitable guest for calix[6]arene **3**, the latter was titrated with **4** in CD_2Cl_2 by ^{1}H NMR. The resulting spectra are reported in Figure 3. A saturation behavior is apparent following the signals related to host **3**. The aromatic singlets of moieties *a* and *b* diverge on increasing concentrations of **4**. In the meantime, the methoxy signals are down-field shifted, and the singlet related to the methylene bridges becomes broader and broader, due to a rigidification of the structure when guest **4** is hosted inside **3**. This loss of conformational flexibility is confirmed by the low-temperature spectra of **3** in presence of a 50-fold molar excess of **4**, with the appearance, at −10 °C, of two doublets for the methylene protons (see SI, Figure S5), typical of a blocked cone conformation of the calixarene.[16] At the same temperature, in the absence of the guest, the methylene protons give a single, slightly broadened signal (see SI, Figure S4). The fit of the experimental points obtained in the titration of **3** with **4** with a 1:1 binding isotherm gives a binding constant K_{ass} of 500 ± 30 M^{-1} with a very nice accordance between the calculated curve and the experimental data (see Figure S3).

Interestingly, along the titration of **3** with **4**, a significant shift of the signals of the guest **4** is also observed. In the first point of the titration (see Figure 3, trace *b*), when added titrant **4** is equimolar to calix[6]arene host **3**, the percentage of added **4** complexed to **3** is significant (38%). Inclusion of guest **4** into the aromatic cavity of host **3** is proved by the marked shielding effect observed on the signals of the guest upon complexation. Under the above conditions, a 0.68 ppm up-field shift is observed on the signal of the methyl group of the guest (δ = 4.61 ppm is the chemical shift of the methyl group of uncomplexed **4**, and δ = 3.93 ppm is the observed chemical shift in trace *b*). Among the aromatic signals related to **4**, that of the alpha proton (H_α) is the most up-field shifted (it is found at 9.30 ppm in trace *b* of Figure 3 as a broad singlet and at 9.95 ppm in uncomplexed **4** as a sharper singlet) indicating that the inclusion must occur as depicted in Figure 2.

Next, we tested the basic properties of calix[6]arene **3** by titration with trifluoroacetic acid (TFA). Addition of the first molar equiv of TFA to a 2.00 mM solution of **3** causes a general down-field shift of all signals due to the protonation of one of the three amino groups (see Figure S6). Further significant variations are observed when a second and a third molar equiv of TFA are added to the solution. In the latter case, most of the signals related to **3** appear broader, and some of them begin to show multiplicity as a consequence of an increased conformational rigidity. ^{1}H NMR spectra (see Figures S6 and S7) do not seem to change appreciably upon subsequent additions of TFA (up to 12 molar equiv). A definite assessment of the protonation state of **3** after the addition of 3 or more molar equiv of TFA is not easy. Doubly protonated $3H_2^{2+}$ with one of the two protons on one of the three amino groups and the other shared between the remaining two amino groups (see Figure 4), or, alternatively, a triply protonated form ($3H_3^{3+}$) with one proton on each of

https://doi.org/10.1021/acs.joc.2c00050
J. Org. Chem. 2022, 87, 3623−3629

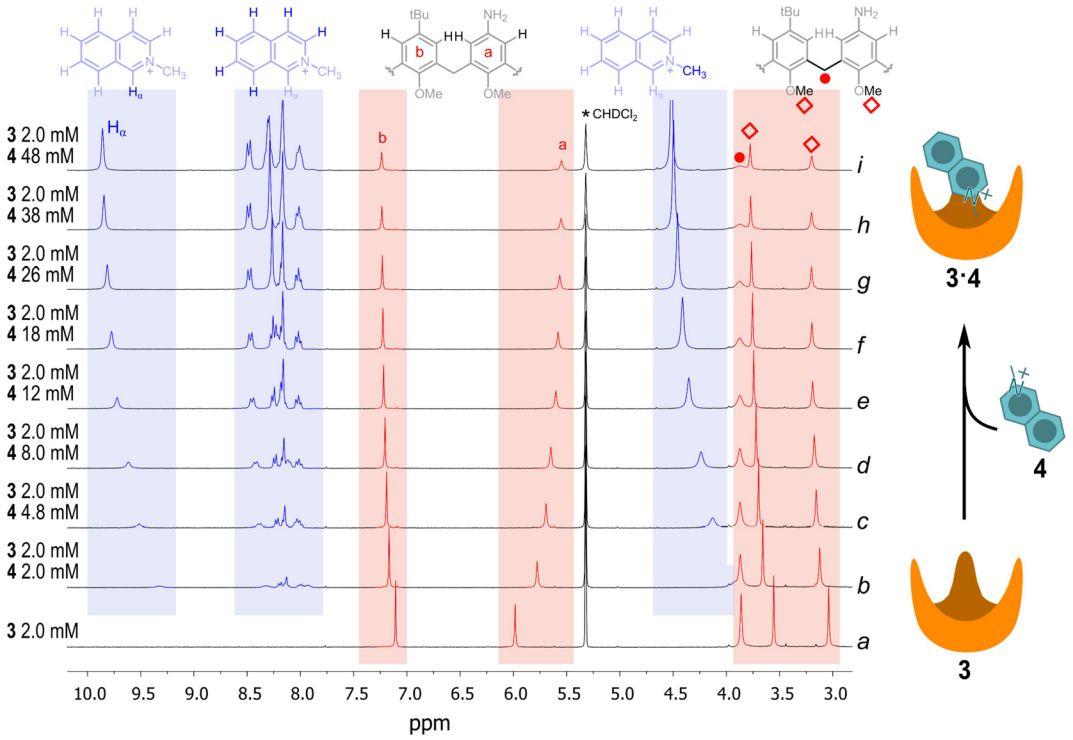

Figure 3. Titration of 2.00 mM calix[6]arene **3** (light red) with **4** (light blue), in CD_2Cl_2 at 25 °C (see Figure S2 for the complete spectra). Trace *a* is related to 2.00 mM calix[6]arene **3**; traces *b*–*i* are related to the same solution to which the given concentration of guest **4** was added (concentration of **3** was maintained constant along the titration).

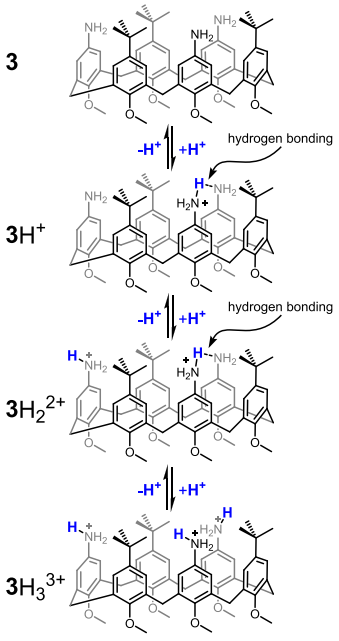

Figure 4. Protonation equilibria involving calix[6]arene **3** in excess of TFA.

the amino groups, could be formed. However, the doubly protonated state $3H_2^{2+}$ seems to be more probable taking into account the following arguments. First, in strict analogy to what was observed in the case of the monoprotonated form of calix[4]arene $2H^+$ (see Figure 1),[9c] the monoprotonated form $3H^+$ obtained by the addition of one molar equiv of TFA to **3** is not deprotonated in any extent by the addition of excess *p*-anisidine up to 20 molar equiv (see Figure S8), proving that **3** has a much more basic character than *p*-anisidine probably due to the chance given to two amino groups to share the proton[17] (see Figure 4). Second, and more importantly, calix[6]arene **3**, differently from *p*-anisidine, is basic enough to promote the decarboxylation of fuel **1d** (*vide infra*). An additional clue in favor of the $3H_2^{2+}$ hypothesis in the presence of 3 or more molar equiv of TFA, comes from the pattern of the methylene bridge signals of the ^{1}H NMR spectrum obtained under these conditions (see Figure S6). They appear as two broad doublets, a typical feature of an almost blocked or slowly interconverting cone conformation. Such conformation is hardly ascribable to a triprotonated $3H_3^{3+}$ structure, which would adjust to keep the three positive groups as far as possible but is fully compatible with the $3H_2^{2+}$ form in which the two protons can be rapidly scrambled among the three amino groups.

Figure 5 shows the effect of protonation on the binding ability of **3** toward *N*-methylisoquinolinium triflate **4**.

Trace *a* is the ^{1}H NMR spectrum of a CD_2Cl_2 solution of 2.00 mM **3** and 6.00 mM **4**. Under these conditions, 70% **3** is in the form of **3**•**4** complex. The addition of 3 molar equiv of TFA causes the complete expulsion of guest **4** from host **3** as can be seen in the resulting trace *b* of Figure 5. Trace *b* is indeed the sum of the ^{1}H NMR spectrum of **4**, trace *c*, and that of **3** + 3 molar equiv of TFA, trace *d*. The reason is probably electrostatic in nature: once host **3** is protonated, it loses any affinity for the positively charged *N*-methylisoquinolinium.

Operation of Receptor 3 under Dissipative Conditions. First of all, we investigated if calix[6]arene **3** is able to promote the decarboxylation of the fuel acids. As expected, it was found that the decarboxylation of acid **1d** (the most activated among 2-cyano-2-phenylpropanoic acids) promoted by **3** occurs in relatively quick times (the reaction is complete

https://doi.org/10.1021/acs.joc.2c00050
J. Org. Chem. 2022, 87, 3623−3629

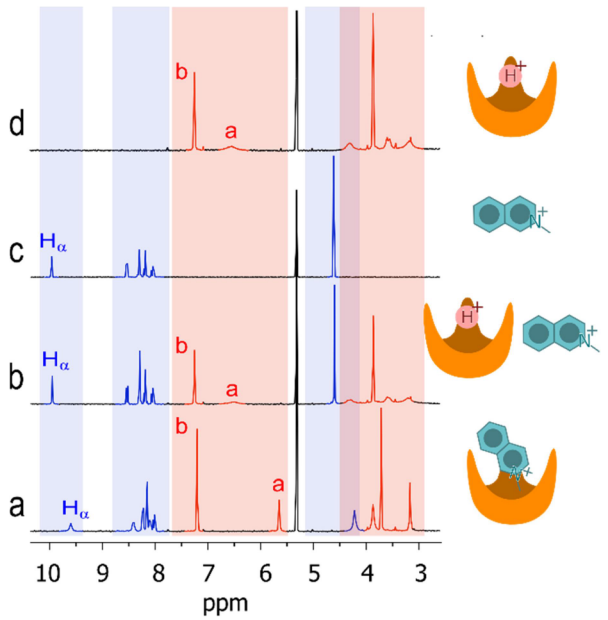

Figure 5. Effect of protonation on the binding ability of **3** (light red) toward *N*-methylisoquinolinium triflate **4** (light blue). (a) 2.00 mM **3** and 6.00 mM **4**; (b) 2.00 mM **3** and 6.00 mM **4** and 6.00 mM TFA; (c) 6.00 mM **4**; (d) 2.00 mM **3** and 6.00 mM TFA. CD_2Cl_2, 25 °C (see Figure S9 for complete spectra). Signal labeling as in Figure 3.

within 6.2 h in CD_2Cl_2 at 25 °C).[18] To an initial 2.00 mM **3** solution (trace *a*, Figure 6a), fuel **1d** (3 molar equiv) is added and **3** is immediately protonated (trace *b*, Figure 6a). Decarboxylation starts and, within 6.2 h, the singlet at 1.75 ppm due to the methyl group of the deprotonated form of **1d**, is transformed into the doublet at 1.60 ppm belonging to the waste product. The typical quartet at 3.95 ppm of the benzylic proton of the waste product also appears (see Figure S10 for a better view).

Contextually, calix[6]arene **3** returns to its original non-protonated form. Interestingly, the reaction does not occur to any extent within the same time when *p*-anisidine (6.00 mM) is added instead of **3**, strongly pointing to the sharing of the proton between two of the three amino groups in $\mathbf{3}H^+$ as a reason for the increased basicity of **3**. The same experiment was then repeated in the presence of 2.00 mM **4**.

Under these conditions, 38% **3** is engaged in the formation of complex **3•4** (trace *a*, Figure 6b). Now, fuel **1d** is added (3 molar equiv with respect to **3**), host **3** is immediately protonated, and guest **4** is released into the bulk solution (trace *b*, Figure 6b). Decarboxylation of the deprotonated form of **1d** slowly occurs, **3** is contextually deprotonated again, and **4** is re-uptaken by host **3** (traces *c*–*f*, Figure 6b). Thus, a release-and-reuptake cycle of guest **4** from and into host **3** has been realized under dissipative conditions (Figure 6c).[19] The process can be satisfactorily reiterated as shown by Figure 6d, where four subsequent cycles triggered by four successive additions of fuel **1d** are monitored by following the variation of the chemical shift of the methyl group of **4** over the time. Unexpectedly, during this release–reuptake experiment (Figure 6b), a second waste product accounting for about 25% of **1d** (Figure 6b, trace *f*, yellow singlet at 1.95 ppm to be compared with the red doublet at 1.60 ppm) appears among the reaction products. Peroxide **5** in Figure 7 was tentatively proposed as this unexpected waste product (see SI, pages S14–S15). It does not form in the absence of **4** (Figure 6a). Furthermore, such a product is not seen when the same

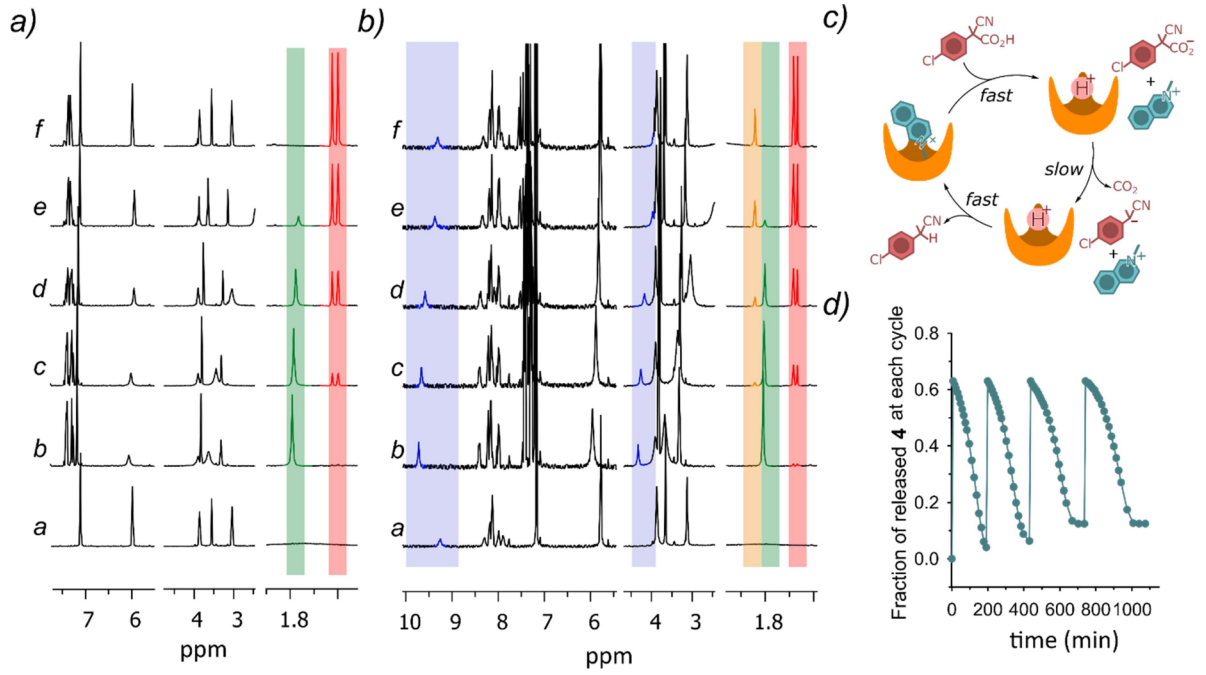

Figure 6. (a) Reaction between 2.00 mM **3** and 6.00 mM **1d** in CD_2Cl_2 at 25 °C followed by ^{1}H NMR (300 MHz); trace *a* was recorded before the addition of **1d**, traces *b*, *c*, *d*, *e*, and *f* were recorded from 6 to 370 min. (b) Reaction between 2.00 mM **3** and 6.00 mM **1d** in the presence of 2.00 mM **4** in CD_2Cl_2 at 25 °C followed by ^{1}H NMR (300 MHz); trace *a* was recorded before the addition of **1d**, traces *b*, *c*, *d*, *e*, and *f* were recorded from 6 to 177 min. (c) Schematic cartoon representing the release–reuptake **3•4** → $\mathbf{3}H^+$ + **4** → **3•4** dissipative cycle driven by fuel **1d**. (d) Four subsequent **3•4** → $\mathbf{3}H^+$ + **4** → **3•4** dissipative cycles triggered by four successive additions of fuel **1d** (in each cycle, 3 mol equiv of **1d** were added to equimolar 2.00 mM of **3** and **4**).

https://doi.org/10.1021/acs.joc.2c00050
J. Org. Chem. 2022, 87, 3623–3629

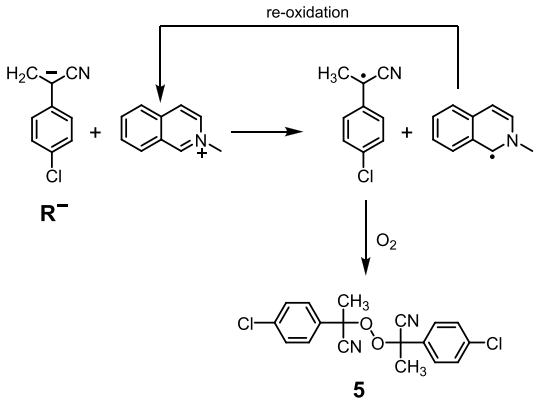

Figure 7. Proposed mechanistic pathway to peroxide **5**.

reaction is carried out in the presence of **4** but substituting **3** with Et_3N (a base able to promote the decarboxylation of **1d**). In other words, it is only formed when calix[6]arene **3** and *N*-methylmethylisoquinolium triflate are both present in the reaction mixture. We hypothesize that it is due to the oxidation of the carbanion by **4**,[9b,20] immediately followed by oxygen capture, see Figure 7. The resulting *N*-methylisoquinoline radical must be then re-oxidized to *N*-methylisoquinolinium (very likely by O_2) since the latter is found untouched at the end of each cycle.

Thus, this collateral pathway, which is somewhat facilitated by calix[6]arene **3**,[21] does not interfere on the release−reuptake cycles. Interestingly, the contribution of the collateral pathway definitely decreases (passing from 25 to 15%) when the exclusion of O_2 from the solution was attempted through freeze−pump−thaw cycles operated on the NMR tube or when higher excesses of fuel **1d**, 10.5 mM (5.25 mol equiv) and 18.4 mM (9.2 mol equiv) were added (passing from 25 to 15 and 10%, respectively), *vide infra*.

Eventually, time control of the dissipative release−reuptake cycle could be achieved by varying the amount of fuel **1d** added in the solution. Figure 8 shows three experiments where increasing amounts of fuel **1d** were added to mixtures of **3** (2.0 mM) and **4** (2.0 mM). The percentage of **4** temporarily escaped from **3** and the time spent outside increase on increasing the amount of the fuel added. When 3 molar equiv of **1d** are added (6.0 mM, Figure 8, yellow points), 63% of the guest is released by the host, and the reuptake process takes 150 min, when 5.25 molar equiv of **1d** are added (10.5 mM, Figure 8, orange points), 75% of **4** is released and reuptake takes 300 min, eventually, when 9.2 molar equiv of **1d** are added (18.4 mM, Figure 8, azure points), 85% of **4** is released and reuptake takes more than 900 min. In other words, the higher the fuel excess, the longer the time needed to consume such excess, the longer the time spent by the host in the unloaded state. The particular shape of the kinetic profiles in Figure 8 (see also Figures S13 and S15) after the exhaustion of excess fuel is probably due to an autocatalytic path involving deprotonated **3** itself as the catalyst. Such complex mechanism has been studied in detail in the simpler case of calix[4]arene **2**.[9c] In that case, it was shown that the fact that the rate of the autocatalytic process does not slow down on decreasing the substrate (fuel) concentration, with the consequent presence of a cusp just before the final plateau, can be explained considering the autocatalytic path to be kinetically zero order with respect to the substrate itself.[9c,22] The presence of minute

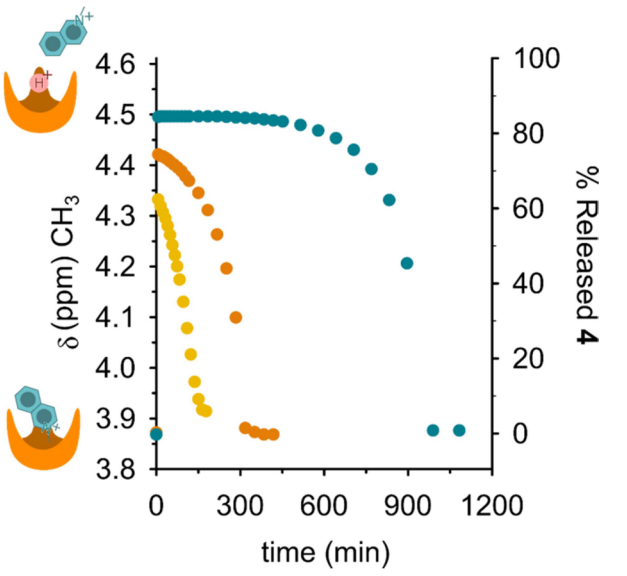

Figure 8. Time-controlled dissipative **3•4** → $3H^+$ + **4** → **3•4** cycles triggered by increasing amounts of fuel **1d** (CD_2Cl_2, 25 °C). In all experiments, equimolar amounts of **3** and **4** were used (2.0 mM) while concentration of **1d** was varied as follows: (1) 6.0 mM (yellow), (2) 10.5 mM (orange) and (3) 18.2 mM (azure). The advancement degree of the reaction over time (right axis) was calculated as $[(\delta - 3.87)/(4.61-3.87)]$, where δ is the chemical shift of the *N*-methylisoquinolium methyl signal (left axis) observed at a given reaction time, 4.61 is the chemical shift of the methyl signal of uncomplexed *N*-methylisoquinolium, and 3.87 is the chemical shift of the *N*-methylisoquinolium methyl signal under the initial conditions, that is, when 38% complex **3•4** formation is observed (which corresponds to 0.76 mM **3•4**).

amounts of cationic impurities in dichloromethane was shown to be likely responsible for such bizarre kinetic behavior.[9c]

CONCLUSIONS

In this report, we have shown that the host−guest interaction between calix[6]arene **3** and *N*-methylisoquinolinium triflate **4** can be dissipatively driven by fuel acid **1d**. The addition of the fuel into a solution containing the complex **3•4** causes the temporary release of guest **4** by the host into the bulk. The former is re-uptaken by the latter once the fuel is exhausted. The amount of released guest and the duration of the unloaded state can be controlled at will by a fine modulation of the quantity of added fuel. Thus, the fully abiotic host−guest couple (**3•4**) described above is capable of operating under dissipative conditions (out of equilibrium, as long as the fuel is present), which are typical, operative conditions of systems with life-like properties.

A possible development of the present work could be the design of systems where the dissipative complex dissociation gives rise to a secondary effect. The temporal control of catalytic activity may be, for example, obtained in case the guest is a catalyst of a given reaction.[23]

ASSOCIATED CONTENT

Supporting Information

The Supporting Information is available free of charge at https://pubs.acs.org/doi/10.1021/acs.joc.2c00050.

Experimental section, ^1H NMR spectra of **4**, ^1H NMR titration experiments, variable temperature ^1H NMR

https://doi.org/10.1021/acs.joc.2c00050
J. Org. Chem. 2022, 87, 3623−3629

spectra of **3** and **3●4**, kinetic experiments, identification of peroxide **5** (PDF)

AUTHOR INFORMATION

Corresponding Authors

Laura Baldini − *Dipartimento di Scienze Chimiche, della Vita e della Sostenibilità Ambientale, Università degli Studi di Parma, Parma 43124, Italy;* orcid.org/0000-0002-0985-4331; Email: laura.baldini@unipr.it

Stefano Di Stefano − *Dipartimento di Chimica, Università di Roma La Sapienza and ISB-CNR Sede Secondaria di Roma - Meccanismi di Reazione, Roma I-00185, Italy;* orcid.org/0000-0002-6742-0988; Email: stefano.distefano@uniroma1.it

Authors

Francesco Rispoli − *Dipartimento di Scienze Chimiche, della Vita e della Sostenibilità Ambientale, Università degli Studi di Parma, Parma 43124, Italy*

Emanuele Spatola − *Dipartimento di Chimica, Università di Roma La Sapienza and ISB-CNR Sede Secondaria di Roma - Meccanismi di Reazione, Roma I-00185, Italy*

Daniele Del Giudice − *Dipartimento di Chimica, Università di Roma La Sapienza and ISB-CNR Sede Secondaria di Roma - Meccanismi di Reazione, Roma I-00185, Italy*

Roberta Cacciapaglia − *Dipartimento di Chimica, Università di Roma La Sapienza and ISB-CNR Sede Secondaria di Roma - Meccanismi di Reazione, Roma I-00185, Italy;* orcid.org/0000-0002-3119-4851

Alessandro Casnati − *Dipartimento di Scienze Chimiche, della Vita e della Sostenibilità Ambientale, Università degli Studi di Parma, Parma 43124, Italy;* orcid.org/0000-0001-9993-3262

Complete contact information is available at: https://pubs.acs.org/10.1021/acs.joc.2c00050

Author Contributions

[§]F.R., E.S., and D.D.G. contributed equally.

Notes

The authors declare no competing financial interest.

ACKNOWLEDGMENTS

S.D.S. thanks University of Rome La Sapienza (Grandi Progetti di Ricerca, Ateneo 2018). F.R., A.C., and L.B. acknowledge the Centro Interdipartimentale Misure "G. Casnati" of Parma University, the BacHound Project (MIUR-PRIN2017 n. 2017E44A9P), and the COMP-HUB Initiative 'Departments of Excellence' (MIUR, 2018−2022).

REFERENCES

(1) (a) Erbas-Cakmak, S.; Leigh, D. A.; McTernan, C. T.; Nussbaumer, A. L. Artificial Molecular Machines. *Chem. Rev.* **2015**, *115*, 10081−10206. (b) Baroncini, M.; Silvi, S.; Credi, A. Photo- and Redox-Driven Artificial Molecular Motors. *Chem. Rev.* **2020**, *120*, 200−268. (c) Das, K.; Gabrielli, L.; Prins, L. J. Chemically Fueled Self-Assembly in Biology and Chemistry. *Angew. Chem., Int. Ed.* **2021**, *60*, 20120−20143. (d) *Out-of-Equilibrium (Supra)molecular Systems and Materials*, Giuseppone, N.; Walther, A. Eds.; Wiley-VHC: Weinheim, 2021.

(2) Biagini, C.; Di Stefano, S. Abiotic Chemical Fuels for the Operation of Molecular Machines. *Angew. Chem., Int. Ed.* **2020**, *59*, 8344−8354.

(3) Some selected examples are: (a) van Rossum, S. A. P.; Tena-Solsona, M.; van Esch, J. H.; Eelkema, R.; Boekhoven, J. Dissipative Out-of-equilibrium Assembly of Man-made Supramolecular Materials. *Chem. Soc. Rev.* **2017**, *46*, 5519−5535. (b) Della Sala, F.; Neri, S.; Maiti, S.; Chen, J. L.-Y.; Prins, L. J. Transient Self-assembly of Molecular Nanostructures Driven by Chemical Fuels. *Curr. Opin. Biotechnol.* **2017**, *46*, 27−33. (c) Pezzato, C.; Cheng, C.; Stoddart, J. F.; Astumian, R. D. Mastering the Non-equilibrium Assembly and Operation of Molecular Machines. *Chem. Soc. Rev.* **2017**, *46*, 5491−5507. (d) Sorrenti, A.; Leira-Iglesias, J.; Markvoort, A. J.; de Greef, T. F. A.; Hermans, T. M. Non-equilibrium Supramolecular Polymerization. *Chem. Soc. Rev.* **2017**, *46*, 5476−5490. (e) Ragazzon, G.; Prins, L. J. Energy Consumption in Chemical Fuel-driven Self-assembly. *Nat. Nanotechnol.* **2018**, *13*, 882−889. (f) Rieß, B.; Grötsch, R. K.; Boekhoven, J. The Design of Dissipative Molecular Assemblies Driven by Chemical Reaction Cycles. *Chem* **2020**, *6*, 552−578. (g) Hossain, M. M.; Atkinson, J. L.; Hartley, C. S. Dissipative Assembly of Macrocycles Comprising Multiple Transient Bonds. *Angew. Chem., Int. Ed.* **2020**, *59*, 13807−13813. (h) Weißenfels, M.; Gemen, J.; Klajn, R. Dissipative Self-Assembly: Fueling with Chemicals Versus Light. *Chem* **2021**, *7*, 23−37. (i) Kariyawasam, L. S.; Hossain, M. M.; Hartley, C. S. The Transient Covalent Bond in Abiotic Nonequilibrium Systems. *Angew. Chem., Int. Ed.* **2021**, *60*, 12648−12658.

(4) Some selected examples are: (a) Yurke, B.; Turberfield, A. J.; Mills, A. P., Jr; Simmel, F. C.; Neumann, J. L. A DNA-fuelled Molecular Machine Made of DNA. *Nature* **2000**, *406*, 605−608. (b) Omabegho, T.; Sha, R.; Seeman, N. C. A Bipedal DNA Brownian Motor with Coordinated Legs. *Science* **2009**, *324*, 67−71. (c) Del Grosso, E.; Ragazzon, G.; Prins, L. J.; Ricci, F. Fuel-Responsive Allosteric DNA-Based Aptamers for the Transient Release of ATP and Cocaine. *Angew. Chem., Int. Ed.* **2019**, *17*, 5582−5589. (d) Heinen, L.; Walther, A. Programmable Dynamic Steady States in ATP-driven Nonequilibrium DNA Systems. *Sci. Adv.* **2019**, *5*, No. eaaw0590. (e) Deng, J.; Bezold, D.; Jessen, H. J.; Walther, A. Multiple Light Control Mechanisms in ATP-Fueled Non-equilibrium DNA Systems. *Angew. Chem., Int. Ed.* **2020**, *29*, 12084−12092. (f) Del Grosso, E.; Prins, L. J.; Ricci, F. Transient DNA-Based Nanostructures Controlled by Redox Inputs. *Angew. Chem., Int. Ed.* **2020**, *59*, 13238−13245. (g) Deng, J.; Walther, A. Pathway Complexity in Fuel-Driven DNA Nanostructures with Autonomous Reconfiguration of Multiple Dynamic Steady States. *J. Am. Chem. Soc.* **2020**, *142*, 685−689. (h) Zhou, Z.; Ouyang, Y.; Wang, J.; Willner, I. Dissipative Gated and Cascaded DNA Networks. *J. Am. Chem. Soc.* **2021**, *143*, 5071−5079. (i) Mariottini, D.; Del Giudice, D.; Ercolani, G.; Di Stefano, S.; Ricci, F. Dissipative Operation of pH-Responsive DNA-Based Nanodevices. *Chem. Sci.* **2021**, *12*, 11735−11739.

(5) (a) Feng, Y.; Ovalle, M.; Seale, J. S. W.; Lee, C. K.; Kim, D. J.; Astumian, R. D.; Stoddart, J. F. Molecular Pumps and Motors. *J. Am. Chem. Soc.* **2021**, *143*, 5569−5591. (b) Canton, M.; Groppi, J.; Casimiro, L.; Corra, S.; Baroncini, M.; Silvi, S.; Credi, A. Second-Generation Light-Fueled Supramolecular Pump. *J. Am. Chem. Soc.* **2021**, *143*, 10890−10894. (c) Amano, S.; Fielden, S. D. P.; Leigh, D. A. A Catalysis-Driven Artificial Molecular Pump. *Nature* **2021**, *594*, 529−534. (d) Feng, L.; Qiu, Y.; Guo, O.-H.; Chen, Z.; Seale, J. S. W.; He, K.; Wu, H.; Feng, Y.; Farha, O. K.; Astumian, R. D.; Stoddart, J. F. Active Mechanisorption Driven by Pumping Cassettes. *Science* **2021**, *374*, 1215.

(6) (a) Wood, C. S.; Browne, C.; Wood, D. M.; Nitschke, J. R. Fuel-Controlled Reassembly of Metal−Organic Architectures. *ACS Cent. Sci.* **2015**, *1*, 504−509. (b) Del Giudice, D.; Spatola, E.; Valentini, M.; Bombelli, C.; Ercolani, G.; Di Stefano, S. Time-Programmable pH: Decarboxylation of Nitroacetic Acid Allows the Time-Controlled Rising of pH to a Definite Value. *Chem. Sci.* **2021**, *12*, 7460−7466.

(7) Ghosh, A.; Paul, I.; Schmittel, M. Multitasking with Chemical Fuel: Dissipative Formation of a Pseudorotaxane Rotor from Five Distinct Components. *J. Am. Chem. Soc.* **2021**, *143*, 5319−5323.

(8) (a) Berrocal, J. A.; Biagini, C.; Mandolini, L.; Di Stefano, S. Coupling of the Decarboxylation of 2-Cyano-2-phenylpropanoic Acid

to Large-Amplitude Motions: A Convenient Fuel for an Acid−Base-Operated Molecular Switch. *Angew. Chem., Int. Ed.* **2016**, *55*, 6997−7001. (b) Ghosh, A.; Paul, I.; Adlung, M.; Wickleder, C.; Schmittel, M. Oscillating Emission of [2] Rotaxane Driven by Chemical Fuel. *Org. Lett.* **2018**, *20*, 1046−1049. (c) Biagini, C.; Di Pietri, F.; Mandolini, L.; Lanzalunga, O.; Di Stefano, S. Photoinduced Release of a Chemical Fuel for Acid−Base-Operated Molecular Machines. *Chem. − Eur. J.* **2018**, *24*, 10122−10127. (d) Biagini, C.; Capocasa, G.; Cataldi, V.; Del Giudice, D.; Mandolini, L.; Di Stefano, S. The Hydrolysis of the Anhydride of 2-Cyano-2-phenylpropanoic Acid Triggers the Repeated Back and Forth Motions of an Acid−Base Operated Molecular Switch. *Chem. − Eur. J.* **2019**, *25*, 15205−15211.

(9) (a) Biagini, C.; Albano, S.; Caruso, R.; Mandolini, L.; Berrocal, J. A.; Di Stefano, S. Variations in the Fuel Structure Control the Rate of the Back and Forth Motions of a Chemically Fuelled Molecular Switch. *Chem. Sci.* **2018**, *9*, 181−188. (b) Franchi, P.; Poderi, C.; Mezzina, E.; Biagini, C.; Di Stefano, S.; Lucarini, M. 2-Cyano-2-phenylpropanoic Acid Triggers the Back and Forth Motions of an Acid−Base-Operated Paramagnetic Molecular Switch. *J. Org. Chem.* **2019**, *84*, 9364−9368. (c) Del Giudice, D.; Spatola, E.; Cacciapaglia, R.; Casnati, A.; Baldini, L.; Ercolani, G.; Di Stefano, S. Time Programmable Locking/Unlocking of the Calix[4]arene Scaffold by Means of Chemical Fuels. *Chem. − Eur. J.* **2020**, *26*, 14954−14962.

(10) (a) Erbas-Cakmak, S.; Fielden, S. D. P.; Karaca, U.; Leigh, D. A.; McTernan, C. T.; Tetlow, D. J.; Wilson, M. R. Rotary and Linear Molecular Motors Driven by Pulses of a Chemical Fuel. *Science* **2017**, *358*, 340−343. (b) Spatola, E.; Rispoli, F.; Del Giudice, D.; Cacciapaglia, R.; Casnati, A.; Marchiò, L.; Baldini, L.; Di Stefano, S. Dissipative Control of the Fluorescence of a 1,3-Dipyrenyl Calix[4]-arene in the Cone Conformation. *Org. Biomol. Chem.* **2022**, *20*, 132−138.

(11) (a) Arduini, A.; Domiano, L.; Ogliosi, L.; Pochini, A.; Secchi, A.; Ungaro, R. Self-Assembled Hydrogen-Bonded Molecular Cages of Calix[6]arenetricarboxylic Acid Derivatives. *J. Org. Chem.* **1997**, *62*, 7866−7868. (b) Arduini, A.; Ferdani, R.; Pochini, A.; Secchi, A.; Ugozzoli, F. Calix[6]arene as a Wheel for Rotaxane Synthesis. *Angew. Chem., Int. Ed.* **2000**, *39*, 3453−3456. (c) Coquière, D.; Le Gac, S.; Darbost, U.; Sénèque, O.; Jabin, I.; Reinaud, O. Biomimetic and Self-Assembled Calix[6]arene-Based Receptors for Neutral Molecules. *Org. Biomol. Chem.* **2009**, *7*, 2485−2500. (d) Lascaux, A.; De Leener, G.; Fusaro, L.; Topić, F.; Rissanen, K.; Luhmer, M.; Jabin, I. Selective Recognition of Neutral Guests in an Aqueous Medium by a Biomimetic Calix[6]cryptamide Receptor. *Org. Biomol. Chem.* **2016**, *14*, 738−746. (e) Tranfić Bakić, M.; Iuliano, V.; Talotta, C.; Geremia, S.; Hickey, N.; Spinella, A.; De Rosa, M.; Soriente, A.; Gaeta, C.; Neri, P. Threading of Conformationally Stable Calix [6] arene Wheels Substituted at the Methylene Bridges. *J. Org. Chem.* **2019**, *84*, 11922−11927. (f) Nyssen, N.; Ajami, D.; Ardelean, A.; Desroches, F.; Li, J.; Luhmer, M.; Reinaud, O.; Jabin, I. Closing a Calix[6]arene-Based Funnel Zn^{2+} Complex at Its Large Rim Entrance: Consequences on Metal Ion Affinity and Host−Guest Properties. *J. Org. Chem.* **2021**, *86*, 12075−12083.

(12) Zahim, S.; Wickramasinghe, L. A.; Evano, G.; Jabin, I.; Schrock, R. R.; Müller, P. Calix[6]azacryptand Ligand with a Sterically Protected Tren-Based Coordination Site for Metal Ions. *Org. Lett.* **2016**, *18*, 1570−1573.

(13) Arduini, A.; Casnati, A. *Macrocycle Synthesis, A Practical Approach*; Parker, D., Ed.; Oxford University Press: Oxford, 1996; pp 145−173.

(14) Bockman, T. M.; Kochi, J. K. Nucleophilic addition versus electron transfer in carbonylmetallate salts. Donor−acceptor interactions in the precursor ion pairs. *J. Phys. Org. Chem.* **1997**, *10*, 542−562.

(15) Gutsche, C. D.; Bauer, L. J. Calixarenes. 14. The Conformational Properties of the Ethers and Esters of the Calix[6]arenes and the Calix[8]arenes. *J. Am. Chem. Soc.* **1985**, *107*, 6059−6063.

(16) Gaeta, C.; Troisi, F.; Neri, P. *endo*-Cavity Complexation and Through-the-Annulus Threading of Large Calixarenes Induced by Very Loose Alkylammonium Ion Pairs. *Org. Lett.* **2010**, *12*, 2092−2095.

(17) In the presence of 1 molar equiv of TFA, the proton could be also shared by all the three amino groups.

(18) Among 2-cyano-2-phenylpropanoic acid derivatives (**1a−d**), 2-cyano-2-(4′-chloro)phenylpropanoic acid **1d** was chosen because its decarboxylation is promoted by calix **3** in convenient times: it is over within 6.2 h under the adopted conditions, thus being complete within one work day. The reaction is slower and less convenient with acids **1a−c**. Decarboxylation of nitroacetic acid is instead too fast to be experimentally convenient under the adopted conditions. Eventually, we prefer to use 2-cyano-2-phenylpropanoic acid derivatives (**1a−d**) rather than trichloroacetic acid for practical convenience. All 2-cyano-2-phenylpropanoic acid derivatives are easy-to-handle solids. Conversely, trichloroacetic acid is a deliquescent, hard to handle and weight solid. We always find very difficult the preparation of a trichloroacetic acid stock solution with an exactly known concentration (see also ref 10b).

(19) No difference of the chemical shift of the ^{1}H NMR signals of the waste product is apparent in the presence or absence of calixarene **3** in all its protonation states, reasonably excluding any inclusion of the waste product into **3**. Little (in no case higher than 0.020 ppm) differences are observed for the signals of the protonated or deprotonated forms of fuel **1d** in the presence or absence of **3**, reasonably excluding inclusion also in this case.

(20) Del Giudice, D.; Tavani, F.; Frateloreto, F.; Di Berto Mancini, M.; Busato, M.; Olivera de Soza, D.; Cenesi, F.; Lanzalunga, O.; Di Stefano, S.; D'Angelo, P. Two Faces of the Same Coin: Coupling X-ray Absorption and NMR Spectroscopies to Investigate the Exchange Reaction Between Prototypical Cu Coordination Complexes. *Chem. − Eur. J.* **2022**, *28*, e202103825.

(21) A hypothetical, tentative explanation is that calixarene **3** may favor the electron transfer between carbanion $\mathbf{R}^-$ and **4** by complexing the transient ion pair $\mathbf{4}\bullet\mathbf{R}^-$ and properly orienting the two species in close proximity.

(22) As pointed out in ref 9c, the observation of a pseudo zero-order substrate dependency for an autocatalytic reaction occurring in homogeneous solution can arise due to one of two possible mechanisms: (i) the autocatalyst is involved in a rate-limiting process preceding the reaction with the substrate; (ii) the substrate is involved in a strong pre-equilibrium binding that saturates a catalytic species present in minute amounts, the resulting complex then reacts with the autocatalyst in the rate-limiting product formation. In this case, as in the case of ref 9c, the autocatalyst is the calixarene in its neutral form and the substrate is the fuel acid. However, if mechanism i were operating, the rate of the autocatalytic process would be independent of the nature of the fuel. Nevertheless, in the case of ref 9c investigation of the kinetics of the reaction with different fuels (2-cyano-2-phenylpropanoic acids, differently substituted at the aromatic ring) showed that the rate of the autocatalytic process is fuel-dependent, thus ruling out mechanism i, and leaving mechanism ii as a viable option.

(23) Li, G.; Trausel, F.; van der Helm, M. P.; Klemm, B.; Brevé, T. G.; van Rossum, S. A. P.; Hartono, M.; Gerlings, H. H. P. J.; Lovrak, M.; van Esch, J. H.; Eelkema, R. Tuneable Control of Organocatalytic Activity through Host−Guest Chemistry. *Angew. Chem., Int. Ed.* **2021**, *60*, 14022−14029.

https://doi.org/10.1021/acs.joc.2c00050
J. Org. Chem. 2022, 87, 3623−3629